GEOSPHERE

GEOSPHERE; v. 15, no. 2

https://doi.org/10.1130/GES01651.1

5 figures

CORRESPONDENCE: paola.vannucchi@rhul.ac.uk

CITATION: Vannucchi, P., 2019, Scaly fabric and slip within fault zones: Geosphere, v. 15, no. 2, https://doi.org/10.1130/GES01651.1.

Science Editor: Shanaka de Silva
Guest Associate Editor: Phillipe Agard

Received 20 December 2017
Revision received 14 October 2018
Accepted 6 December 2018

Scaly fabric and slip within fault zones

Paola Vannucchi[1,2]

[1]Department of Earth Sciences, Royal Holloway, University of London, Egham TW20 0EX, UK
[2]Dipartimento di Scienze della Terra Università di Firenze, 50121 Firenze, Italy

ABSTRACT

Scaly fabric was first described early in the development of geology and has experienced a recent renaissance with the realization that it may play a key role in the shallow coseismic deformation of plate boundary faults, such as the M9 Tohoku-Oki megathrust event. The fabric itself is an anastomosing network of polished surfaces. It is often present in clay-rich sediments deformed by pure and/or simple shear. The faults where it is found typically have multiple modes of slip, from creep to tremor to seismic slip. It is a macroscopic, multi-scale structure that has, to date, been impossible to create under laboratory conditions. In this paper, I review the state of the art of our understanding of this fabric, its mechanical modes of deformation, and its capacity for both aseismic and seismic slip. I also summarize the challenges we face to understand its full importance in the evolution of plate boundary faults. The conclusion is that scaly fabric is linked to frictional-viscous shear zones where bulk viscous deformation is accompanied by localized shear—a condition typical of frictional transition zones in faults.

INTRODUCTION

Scaly fabric describes an array of pervasively anastomosing surfaces where phyllosilicate-rich rocks split into progressively smaller flakes. The surfaces are polished and commonly striated. In fault zones, scaly fabric is classically associated with slow, distributed deformation by shear in underconsolidated clay-rich sediments deforming at low confining pressure (Cowan, 1985; Moore et al., 1986). Its occurrence in the shallowest, creeping sections of faults (Moore et al., 1986; Vannucchi et al., 2003; Maltman and Vannucchi, 2004; Schleicher et al., 2010) is consistent with strain released as aseismic slip.

However, little is effectively known about slip distribution within scaly fabric, and some recent findings and experiments seem to point toward a whole range of situations where scaly fabric can develop and, when developed, influence successive deformation. Recently, for example, clay-rich sediments deformed by scaly fabric were recovered during Integrated Ocean Drilling Program (IODP) Expedition 343, which drilled the plate boundary fault offshore Japan in the area of the coseismic shallow slip induced by the 2011 M9 Tohoku-Oki earthquake (Fujiwara et al., 2011; Ito et al., 2011; Satake et al., 2013). There, the cored décollement is marked by well-developed scaly fabric cut by sharp surfaces of slip (Chester et al., 2013; Kirkpatrick et al., 2015). Based on friction experiments on the clay-rich sediments cored from the décollement interval, IODP Expedition 343 shipboard scientists concluded that scaly fabric and the discrete faults formed respectively by distributed (aseismic) and localized (seismic) slip in the décollement (Kirkpatrick et al., 2015). These experiments revealed that a key parameter controlling the décollement's strength was pore-fluid pressure (Ujiie et al., 2013). At high strain rates, thermal pressurization of pore fluids (sensu Rice, 2006) could have decreased the effective normal stress, and the volume of comminuted particles could have been mobilized through fluidization (Ujiie et al., 2013). Fluidization, however, was not observed along the recovered surfaces of localized slip (Kirkpatrick et al., 2015), and the experiments were not conducted on the scaly clays themselves but on disaggregated samples (Ujiie et al., 2013). A different set of experiments conducted at subseismic slip rates—10 μm/s—on fluid-saturated samples shows that the coefficient of friction of intact fault material from the Tohoku megathrust—i.e., with scaly fabric—is generally low, but higher than in powdered gouges, while their cohesion is negligible (Ikari et al., 2015b).

Scaly fabric has also been recently evoked in the efforts to associate the low-frequency range of slip behaviors of megathrusts, such as episodic tremors and slip (Walter et al., 2013; Saffer and Wallace, 2015; Wallace et al., 2016; Wallace et al., 2017), to actual geological structures. Fossil megathrusts or splay faults show pervasive veins interpreted as cyclic hydrofractures formed and cemented at seismogenic depths within the plate interface (Vrolijk et al., 1988; Brantley et al., 1997; Matsumura et al., 2003; Kondo et al., 2005; Vannucchi et al., 2010; Fagereng et al., 2011; Hashimoto et al., 2012) and within the time scales associated with the recurrence of low-frequency slip instabilities (Fisher and Brantley, 2014). Another common characteristic within these fossil megathrusts and splay faults is the sheared, stratally disrupted nature of the host rock where scaly fabric is developed within the matrix (Byrne, 1984; Vannucchi et al., 2010; Fagereng, 2011; Elliott et al., 2017; Ramirez et al., 2017). Since each hydrofracturing event is accompanied by an increment of simple shear, the crack openings recorded by veins are a direct response to slip on adjacent microfaults within the rock matrix (Fisher and Brantley, 2014). In this scenario, scaly fabric, with its distributed shear on many slip surfaces, large slip distances, and a strain hardening process on individual features, would be one example of direct evidence for slow slip and quasi-dynamic fault motion (Fisher et al., 2017; Ujiie et al., 2018).

The two examples described above suggest that scaly fabric in fault zones may play a critical role in slip distribution. Whether scaly fabric is the direct product of different slip modes, or whether its occurrence changes the shear strength and/or cohesion of the fault zone is still debated. Except for high-strain rotary shear experiments that reproduced an equivalent (mylonitic) fabric in halite-kaolinite simulated gouge (Bos and Spiers, 2000, 2002; Bos et al., 2000), an experimental foundation for the origin and evolution of scaly fabric is still lacking. So, even after almost 200 years after the first description of scaly fabric (Bianconi, 1840), this structure remains elusive, and the influence of scaly fabric on slip concentration remains an unresolved question. Here we review the state of the art on scaly clays and explore a new approach for characterizing its role in the evolution of shear strength at shallow depths in subduction zones at the front of the seismogenic zone.

WHAT IS SCALY FABRIC?

Scaliness ("scagliosita") was defined almost two centuries ago as "polished anastomosing surfaces that penetratively cut through the rock body at the centimeter to millimeter scale" (Bianconi, 1840) (Fig. 1). Scaly surfaces define relatively undeformed, almond-shaped elements of rock called phacoids (Moore et al., 1986) (Figs. 1A and 1B). Phacoids are a few tens of mm in size and may be broken into continually smaller scaly fragments (Fig. 1C). The alignment of phacoids defines a pervasive foliation that is called scaly fabric. Scaly fabric develops in phyllosilicate-rich rocks, and it is commonly developed in both clay-rich sediments (Vannucchi et al., 2003) and serpentinite (Shervais et al., 2011) (Fig. 1). Scaly fabrics can be the product of different processes (Vannucchi et al., 2003):

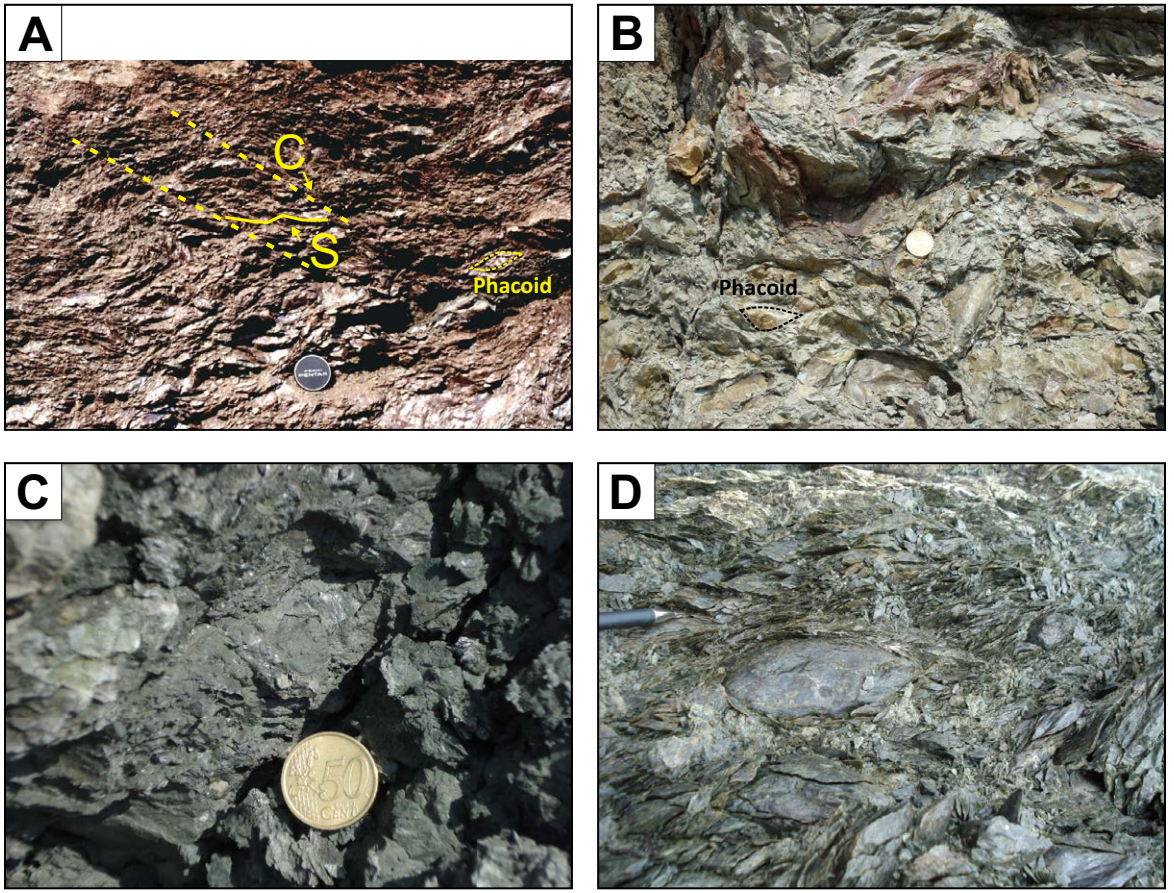

Figure 1. Examples of scaly fabric from type localities in the Northern Apennines and California. (A) Photograph of scaly fabric developed in Argille Varicolori of the Northern Apennines (Baiso, Italy, 44°30′34.69″N–10°37′29.31″E). The scale-like chips are called phacoids. Pervasive foliation is defined by aligned phacoids distributed throughout the clay. This is the only example of the ones presented in this figure where phacoids are arranged following an S-C fabric (yellow dashed lines: C—surcaes; yellow line: S—surface. (A) Phacoids are also shown. (B) Photograph of scaly fabric in Argille Varicolori of the Northern Apennines (Roteglia, Italy, 44°29′59.88″N–10°40′7.09″E). Here the phacoids are not preferentially aligned, but they are rather chaotically oriented. (A) Phacoids are shown. (C) Photograph showing detail of the polished surfaces and the scale-independent character of the phacoids (Argille Varicolori, Baiso, 44°30′34.69″N–10°37′29.31″E). (D) Photograph of scaly fabric developed in serpentine (Franciscan Mélange, Skaggs Creek Road, U.S., 38°42′43.03″N–122°59′43.37″W).

(1) Scaly clays can form by *sedimentary processes*, when gravitational instability of slopes disrupts phyllosilicate-rich deposits, producing mass wasting, such as debris flows.
(2) Scaly fabric can form *tectonically* in response to volumetrically diffuse shear strain—as in broken formations and mélanges or fault zones.
(3) Phyllosilicate-rich sediments that are forced upwards—as a result of tectonic and/or lithostatic stress—and that form *diapirs and mud volcanoes* can develop scaly fabric.
(4) Finally, scaly fabric can develop as a result of *mineral alteration processes*, producing phyllosilicates and volume expansion in a confined rock volume, such as during the serpentinization of peridotites (Shervais et al., 2011).

The different genesis, but also the varying nature of the clay-rich material (different mineralogy, different compaction and/or diagenesis, and different physical properties), as well as the varying intensity of deformation, create the typical issue of dealing with scaliness: that a variety of shapes and arrangements of phacoids coexists within the general definition of scaly fabric (Vannucchi et al., 2003). Even within the scaly fabric developed in clay-rich sediments in relation to faults, which is the focus of this paper, there can be microstructurally distinct types of scaliness associated with different assemblages of structures diagnostic of different deformation mechanisms (e.g., pressure-solution seams, fractures, and shear surfaces). The microscopic characteristics of fault-related scaly fabric will be discussed in the following paragraph; however, it is worth stressing that according to Bianconi's definition, scaly fabric should only describe the mesoscale fabric of specimens, and it is not linked to any specific mechanism or conditions of deformation, such as temperature, depth range, etc. (Agar et al., 1989; Vannucchi et al., 2003).

Scaly Fabric and Décollements—And a Couple of Other Examples

Interestingly, scaly fabric is the deformation structure found in modern décollements drilled at shallow depth between 2 and 10 km inboard from the frontal thrust (Maltman and Vannucchi, 2004; Chester et al., 2013) (Fig. 2).

The Nankai basal décollement, entirely developed within the Lower Shikoku Basin Unit, was cored at ~950 mbsf by Ocean Drilling Program (ODP) Leg 131, where it is ~20 m thick (Taira et al., 1991). The décollement there is sharply

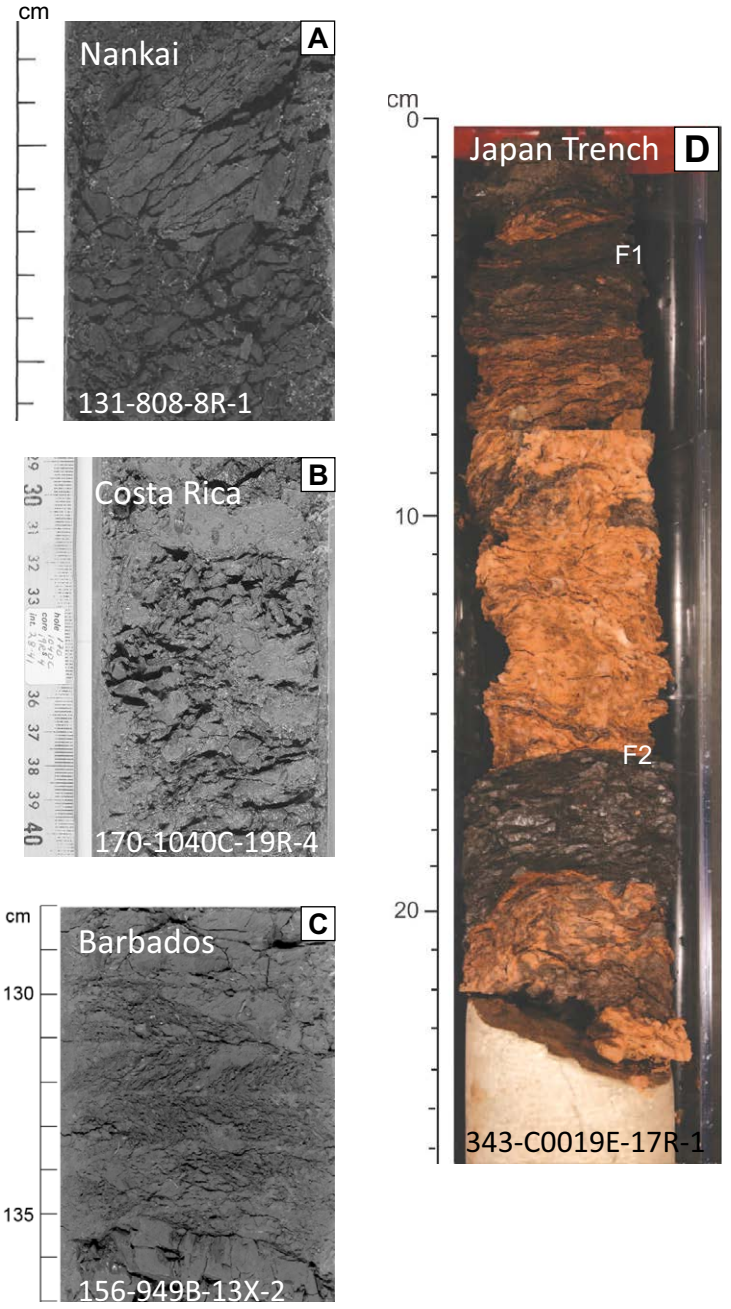

Figure 2. (A) Core photograph of the base of the Nankai décollement drilled during Ocean Drilling Program (ODP) Leg 131 (32°21′6.17″N–134°56′36.96″E). (B) Core photograph of an interval of intact scaly fabric along the Costa Rica décollement, ODP Leg 170 (9°39′41.81″N–86°10′44.10″W). (C) Core photograph of scaly fabric developed in the Barbados décollement cored during ODP Leg 156 (15°32′11.88″N–58°42′50.85″W). (D–G) Whole round core photograph of the Japan Trench décollement drilled during Integrated Ocean Drilling Program (IODP) Expedition 343 (37°56′22.80″N–143°54′38.12″E). In D, F1 and F2 refer to the surfaces of localized slip described by Kirkpatrick et al. (2015).

bounded both at the top by an increase of brecciation and at the bottom, where a 0.15-m-thick scaly fabric zone marks the abrupt base (Maltman et al., 1993) (Fig. 2A). It is interesting to note that scaly fabric was also observed along the Nankai frontal thrust (Moore et al., 2001).

The Costa Rica décollement was successfully drilled by ODP Legs 170 and 205 at ~350 mbsf (Kimura et al., 1997; Morris et al., 2003). The Costa Rica décollement was marked by a gradual increase of brecciation, although drilling disturbance obliterated most of the original deformation (Vannucchi and Tobin, 2000; Tobin et al., 2001). Scaly fabric was only present in some rare intact pieces within the Costa Rica décollement (Fig. 2B). Deformation culminated in a 5-cm-thick zone of plastic deformation identified as the principal surface of slip as well as the bottom boundary of the décollement (Vannucchi and Leoni, 2007).

The Barbados basal décollement was cored during ODP Leg 110 at ~500 mbsf, where it is marked by a sharp increase of scaly fabric intervals that become dominant at the base of an accretionary prism where 10–40-cm-thick layers of scaly clays are present throughout (Mascle et al., 1988). This interval is ~30 m thick with unevenly distributed zones of intense scaly fabric ranging from ~1 to ~2 m thick (Labaume et al., 1997b; Maltman et al., 1997) (Fig. 2C). In Barbados, the ~3.5-m-thick interval containing the "lithological" boundary between accreted and underthrusted sediments is a relatively weakly deformed zone.

The most recent décollement coring was at the Japan Trench in the rupture area of the 2011 M9 Tohoku-Oki earthquake. IODP Expedition 343 of the Japan Trench Fast Drilling Project (JFAST) drilled the décollement a year after its rupture (Chester et al., 2012). The fault zone is thought to have accommodated 50 m of coseismic slip (Fujiwara et al., 2011; Ito et al., 2011; Satake et al., 2013). JFAST recovered ~1 m of shear zone at ~820 mbsf (Chester et al., 2013). The shear zone was found within a single core, and neither its upper nor lower boundaries were recovered. If the entire nonrecovery interval comprised the décollement, then it would have a maximum thickness of ~5 m, in agreement with the logging-while-drilling (LDW) analyses. Lithostratigraphic considerations and comparisons with the incoming sediment sections drilled at Deep Sea Drilling Project (DSDP) Site 436, however, suggest that the maximum width of the plate boundary fault could reach ~15m (Kirkpatrick et al., 2015). Most of the recovered core is composed of clay with variably intense scaly fabric (Fig. 2D). Primary bedding appears to have been completely destroyed by the shear deformation.

Although the Nankai, Costa Rica, Barbados, and Tohoku clay-rich sediments showed in Figure 2 are all described as characterized by scaly fabric, their scaliness is visibly of different "intensity." This effect can indeed be the result of deformation occurring at varying levels of intensities, or it can be related to the nature of the sediments (different mineralogy, different compaction and/or diagenesis, or different physical properties). However, according to Bianconi (1840), they all show the four characteristics typical of scaly fabric—polished, anastomosing, and penetrative surfaces visible at the cm to mm scale.

Another lithospheric-scale fault where scaly fabric was retrieved is the San Andreas fault drilled during the San Andreas Fault Observatory at Depth (SAFOD) project. The SAFOD drillhole is located in central California, where the San Andreas fault has a creep rate of 2.5–3.9 (Titus et al., 2006), and microearthquakes of Mw 0–2.0 are detected at depth of 2–3 km (Nadeau and McEvilly, 2004). The core of the San Andreas fault was successfully drilled and cored at ~3300 m depth (Schleicher et al., 2010). Foliated fine-grained shaly fault rock samples characterized by scaly fabric and abundant polished fracture surfaces were collected from shear zones in and outside the active creeping section of the fault (Schleicher et al., 2010).

Some of the examples of scaly fabric in this review also come from the broken formations of the Argille Varicolori and Argilliti a Palombini of the Northern Apennines (Vannucchi and Bettelli, 2002; Bettelli and Vannucchi, 2003) (Figs. 1A–1C). Although not part of a décollement, these two formations are intensely folded (Bettelli and Vannucchi, 2003), and they developed scaly fabric to accommodate differential slip between carbonaceous and clay-rich layers or limb thinning (Vannucchi et al., 2003). These are also the classic formations of the "Argille Scagliose," where Bianconi (1840) described scaly fabric for the first time.

Mesoscopic to Microscopic Characteristics of Scaly Fabric and Their Structural Associations

Ductile versus Brittle Deformation: Mesoscopic to Microscopic Observations

Mesoscopic and microscopic observations regard scaly fabric as the product of a wide range of processes ranging from dislocation creep, dissolution-precipitation, and particulate flow to sediment failure due to an increase in deviatoric stress and fluid pressure (Moore et al., 1986; Vannucchi et al., 2003; Schleicher et al., 2010). Microscopic observations show that scaly fabric is formed by three types of elementary features created under conditions that span from brittle to ductile processes: flattening bands and/or dissolution surfaces, fractures, and shear surfaces (Prior and Behrmann, 1990; Labaume et al., 1997b) (Fig. 3). These features can occur alone or in combination, such as in the S-C fabric described later. Flattening bands and/or dissolution surfaces develop as a result of processes ranging from diagenetic compaction to pure shear, and they localize strain in mm- to μm-thick layers (Labaume et al., 1997b) (Fig. 3A). Pressure solution can eventually accommodate compaction as a cleavage-forming process (Gratier et al., 2011; Fagereng and den Hartog, 2017). Fractures are sharp surfaces that can develop associated with high fluid pressure (Moore et al., 1986), dilational failure (Prior and Behrmann, 1990), or both. Dilational failure occurs with no or very limited amounts of particle reorientation and has no kinematic indicators (Fig. 3B). Dilation perpendicular to the fracture walls is commonly due to rebound—the release of residual strain and/or stress during unloading—or to contraction due to diagenetically triggered volume loss within the host sediments, such as desiccation (Prior and Behrmann, 1990). Shear surfaces develop from progressive simple shear

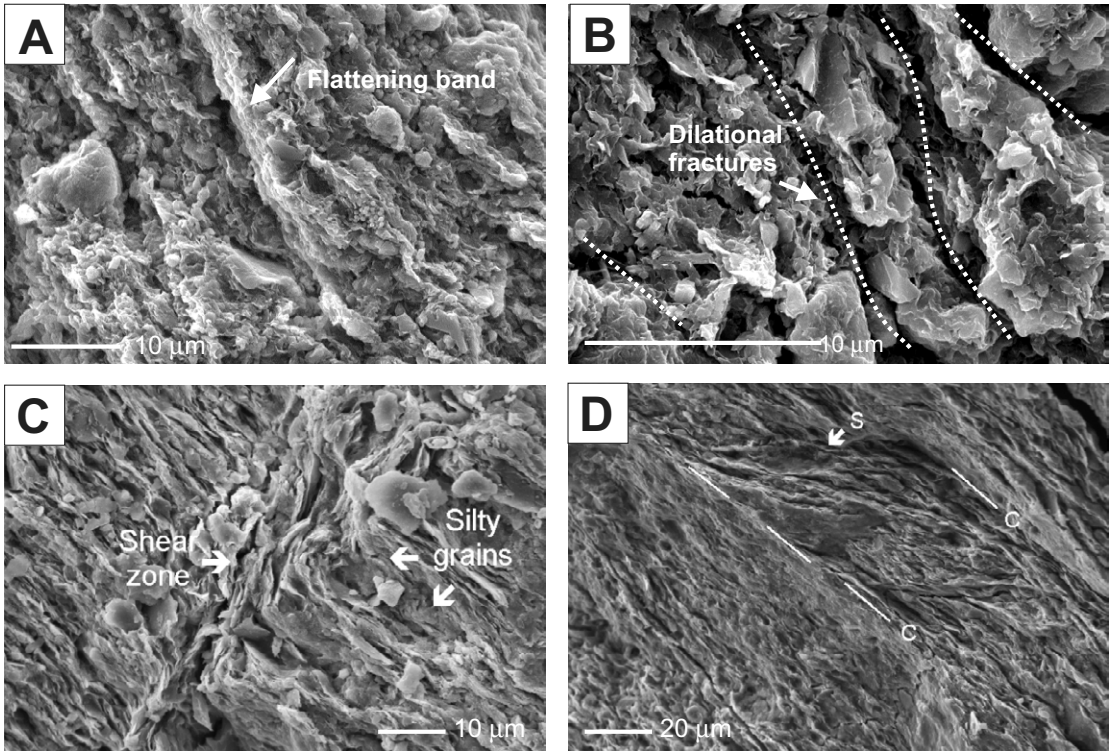

Figure 3. Photomicrographs of samples characterized by scaly fabric. (A) Scanning electron microscope (SEM) secondary mode image showing flattening bands. Porosity reduction is easily visible, while there are no signs of simple shear deformation nor pressure solution—Costa Rica Site 205—1040 décollement (9°39′41.81″N–86°10′44.10″W). (B) SEM secondary mode image showing phacoids delimited by well-developed dilational fractures (dotted lines). Here there is no clay-mineral–preferred orientation in the bulk of the sample nor along the parting surfaces, although there is scaly fabric on the mesoscopic sample—Costa Rica Site 205—1040 décollement (9°39′41.81″N–86°10′44.10″W). (C) SEM secondary mode image showing well-developed and homogeneous-preferred orientation of the platy minerals parallel to bedding cut almost perpendicular by a narrow shear zone—Argille Varicolori involved in Apennine detachment faults (Futa Pass to Mount Falterona tunnel, Firenze; 44° 5′41.70″N–11°16′31.50″E). (D) SEM secondary mode image showing a shear zone with internal S-C geometry cutting at low angle to a well-developed bedding-parallel foliation. Note that the phacoids defined by the intersection of S and C surfaces maintain a preferential orientation of the platy minerals parallel to the background foliation—Argille Varicolori involved in Apennine detachment faults (Futa Pass to Mount Falterona tunnel, Firenze; 44° 5′41.70″N–11°16′31.50″E).

and can show evidence of ductile flow or frictional slip (Moore et al., 1986; Labaume et al., 1997b) (Fig. 3C). In this latter case, lineations on the slip planes can be common (Schleicher et al., 2006; Dellisanti et al., 2008).

In fault zones, the pattern shown by scaly fabric often resembles an S-C fabric, where the S-surfaces are flattening bands and/or dissolution surfaces, and C-surfaces are shear surfaces. Defined for the first time to describe mylonites (Lister and Snoke, 1984), S-C surfaces are also common in shear zones deforming clay-rich sediments (Fig. 3D). C-surfaces (from French *cisaillement*) are usually long, straight, and parallel to the shear zone boundary, sharing also the same sense of dislocation. S-surfaces (from French *schistosité*) are oblique, leaning over in the direction of shear, and make an angle of <45° to the shear plane or shear zone boundary. Displacement is localized on C-surfaces, while the foliation S-surfaces do not record the total shear strain of the rock. The combination of S- and C-surfaces forms the S-C fabric bands ranging from ~1 cm to a few mm. When developed, the S-C bands are usually subparallel to the boundaries of the macroscopic scaly fabric. The C-surfaces are sharp, and the parting of the sediment is easier along them, while the oblique S-surfaces are generally more pervasive.

At the µm scale of observation achievable with scanning electron microscope (SEM) and transmission electron microscope (TEM), planar surfaces defined by preferential orientation of clay minerals show an increase in the face-face contacts between adjacent grains (Bennett et al., 1991) (Fig. 3). This configuration is attained through rotation and slip typical of grain-boundary sliding achieved through particulate flow, and also dislocation glide. These processes produce microstructural domains with discrete zones of locally aligned clay particles, as well as kinked and folded grains. In fact, at the µm scale, the C-surfaces correspond to shear surfaces with a high degree of particle orientation in the direction parallel to slip (Labaume et al., 1997b; Schleicher et al., 2006; Dellisanti et al., 2008). Smaller-size clay minerals can be present on the shear surfaces, and this has been proposed to be an effect of authigenesis (Schleicher et al., 2010), disruption of clay aggregates (Moore et al., 1986), or grain comminution (Casciello et al., 2004). Both of these latter features are associated with increasing confining pressure, and according to fluid-pressure and strain-rate conditions, clay particle size reduction will eventually dominate over particulate flow (Borradaile, 1981). Rotary shear experiments on smectite-rich material showed that grain reduction through cataclasis, wear, and

mechanical amorphization—and in this latter case, the consequent production of amorphous nanoparticles—seems to be directly correlated with high frictional work occurring at relatively low slip rates ≤0.1 m/s and associated to slip strengthening (Aretusini et al., 2017). In this case, higher work could therefore induce strain delocalization and thickening of shear zones, a characteristic of fault zones where scaly fabric is developed.

S-surfaces develop by rotation of particles, involving both particle sliding and bending; this rotation follows porosity collapse. S-surfaces are therefore consistent with a flattening fabric developing between shear surfaces. With increasing confinement, particles along the S-surfaces start to show some internal deformation, such as folding. In this case, particles did not flow independently from each other, and internal particle deformation occurred simultaneously with inter-particle deformation according to a "controlled" or even cataclastic particulate flow (sensu Borradaile, 1981). Shear-strain increase will decrease the angle between C- and S-surfaces in the direction of bulk shear (Labaume et al., 1997b). Within the phacoids defined by the S-C fabric, the sediment domains can be undeformed (Prior and Behrmann, 1990), or they can show alignment of clay particles (Labaume et al., 1997b) particularly toward the edges (Dellisanti et al., 2008). Undeformed volumes of clay particles can be present next to domains where particles are preferentially oriented.

At the mesoscale, polishing is present on both C- and S-surfaces. At the microscale, most studied polished surfaces result from the extreme alignment of clay minerals during slip (Moore et al., 1986; Vannucchi et al., 2003). They can also result from mechanical abrasion (Dellisanti et al., 2008) and new mineral phases (Schleicher et al., 2010). The latter were observed through microscopic work done on scaly fabric samples collected during the SAFOD experiment, wherein the phacoids show a coating of neocrystallized smectite minerals along the shear surfaces (Schleicher et al., 2010).

Scaly Fabric Intensity and Surfaces of Localized Slip

Independent of the scale of observation, if the entire volume of sediments is penetratively foliated, the intensity of scaly fabric is associated with: (1) the relative spacing of polished surfaces and size of phacoids and/or clay-mineral particles; and (2) the angular relationship between C- and S-surfaces. This framework implies that a macroscopic scaly fabric zone has a tendency to evolve from a zone of discontinuous deformation with clay rotation localized in narrow (a few μm to mm) discrete bands, to progressively thicker zones with penetrative S-foliation, to closely spaced, small-size S-C bands and/or phacoids. Shear-related localization of strain may then further align the phacoids and sharp surfaces, and faults can develop to accommodate displacement.

In the core recovered from the décollement in the rupture area of the 2011 M9 Tohoku-Oki earthquake, sharp contacts separating different fabric domains were interpreted as surfaces of localized shear (Chester et al., 2013; Kirkpatrick et al., 2015) (Fig. 2D). Even though no clear correlation between those surfaces and the 2011 Tohoku-Oki earthquake was established, their mesoscopic and microscopic appearance reveals the relationship between scaly fabric and the range of localized shear.

Kirkpatrick et al. (2015) accurately describe the geometry of the scaly fabric in relation to the surfaces of localized slip. In the first case (F1 in Fig. 2D), the fault is a ~1-cm-thick zone where the scaly fabric is gradually crosscut and locally obliterated by brecciation. The fault is subparallel to the S-surfaces in the scaly fabric on both sides. In the second case (F2 in Fig. 2D), the fault develops as a sharp, undulate surface that truncates the preferential orientation of bands, and scaly fabric long axes are at different orientations on either side of the fault. At the microscale, this second fault consists of three submillimeter-thick layers separated by sharp boundaries. Inside each layer, clay grains define a microscopic foliation that gets deflected consistently with the sense of shear across the scaly fabric. So, even though the faults locally crosscut the scaly fabric, the surfaces of localized shear are kinematically compatible with the scaly fabric, and they show no evidence of fluidization.

Similarly to the cores from the Japan Trench décollement, outcrops of scaly clays in the Northern Apennines show geometrical relationships between localized slip and scaly fabric. In the Northern Apennines, concentrated slip appears to develop at different scales in the scaly clays—from surfaces that extend for a few tens of mm to several tens of m (Vannucchi et al., 2003) (Figs. 4A and 4B). Their relationship with the scaly foliation varies from subparallel to oblique (Figs. 4A–4D), similar to what has been observed in the Japan Trench cores. Interestingly, faults are involved in subsequent folding, indicating that viscoplastic deformation resumes after faulting (Fig. 4E).

Scaly Fabric-Vein Association

In modern décollements, scaly fabric can also be associated with veins. In Barbados, in particular, extensional carbonate veins are found parallel to the scaly fabric S-foliation (Fig. 5A). Both the microstructures and chemical features indicate that vein formation there is controlled by hydrofracturing (Labaume et al., 1997a; Maltman et al., 1997). This geometry indicates cyclic variations of the strain regime probably controlled by variations of fluid pressure associated with variation of permeability. Compactional shear strain is active during the formation of scaly fabric, lowering the permeability and increasing pore-fluid pressure; high pore pressure favors hydraulic dilatancy of preexisting discontinuities (the S-surfaces) and transient increase of permeability, followed by dilation and vein mineralization (Moore et al., 1986; Labaume et al., 1997a). This cyclical strain variation is similar to the fault-valve behavior described by Sibson (1990). In the Northern Apennines, scaly fabric is commonly accompanied by a mesh of shear veins and/or faults and dilational jogs. Microstructural observations show 10–100 μm growth increments of the calcite vein through a crack-and-seal process interpreted as repeated episodic overpressure events similar to Barbados (Vannucchi et al., 2010) (Fig. 5B). In the Apennines, stable isotopes on the crack-seal veins show circulation of fluids that originate from deeper horizons along the fault (Vannucchi et al., 2010).

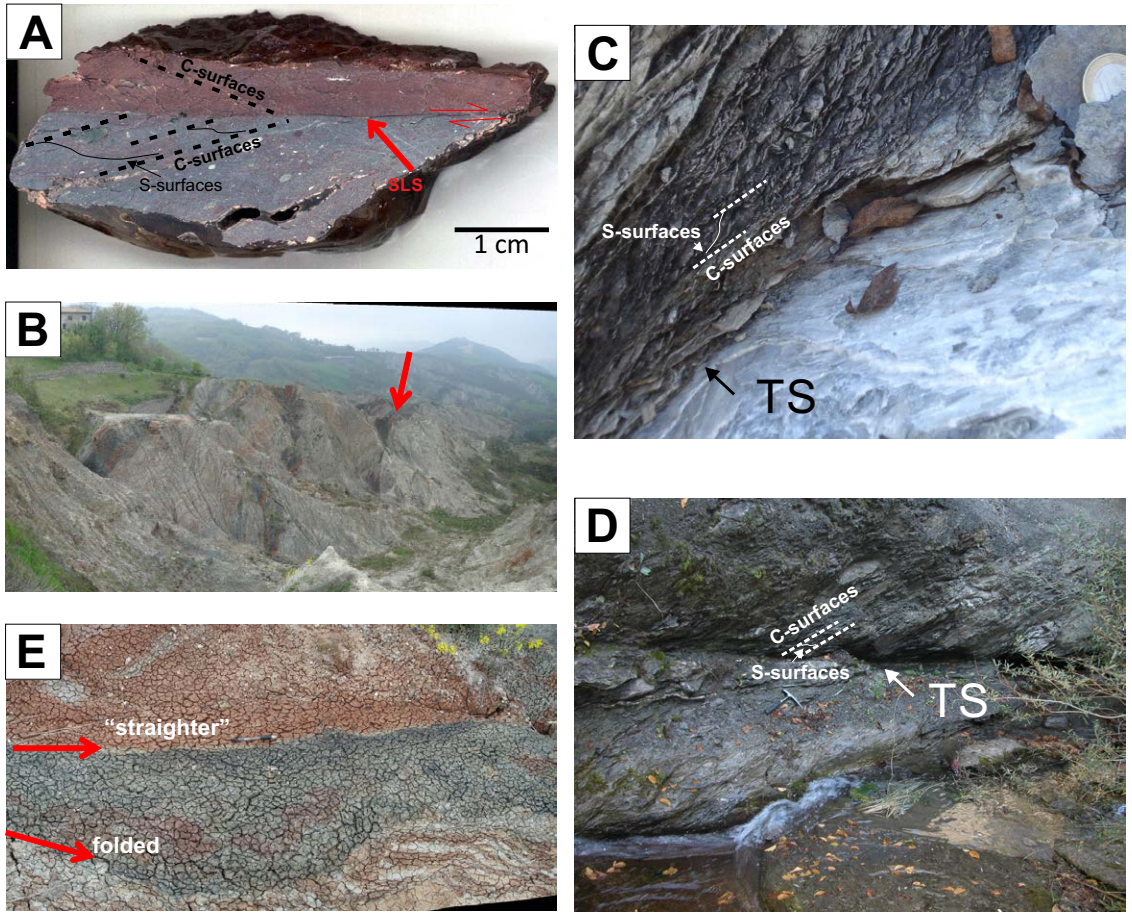

Figure 4. Examples of different relationships between localized slip and scaly fabric—from subparallel to high angle—visible at different scales and their deformation—from straight to folded—from the Northern Apennines (Italy). (A) Photograph of a surface of localized slip cutting at high angle the scaly fabric on both sides of the fault (SLS—surface of localized slip; dashed lines follow C-surfaces; arrow points to S-surfaces). Note that in the coarser-grained gray material on the right, scaly fabric is poorly developed, while the C-surfaces in the red material show evidence of cataclasis, and the S-surfaces are not visible because of how the sample has been cut (Baiso, Italy; 44°30′34.69″N–10°37′29.31″E). Photograph by F. Remitti (University of Modena and Reggio Emilia). (B) Relatively younger fault of undetermined displacement cutting through a clay-rich formation characterized by scaly foliation (Baiso, Italy; 44°30′34.69″N–10°37′29.31″E). (C) Example of a regional thrust surface developed subparallel to the scaly foliation (TS—thrust surface; dashed lines follow C-surfaces; arrow points to S-surfaces) (Vidiciatico, Italy; 44°10′15.63″N–10°51′42.70″E). (D) Example of a regional thrust surface developed at high angle to the scaly foliation, which is decreasing in size from the top-left corner toward the bottom-right (TS—thrust surface; dashed lines follow C-surfaces; arrow points to S-surfaces) (Gova, Italy; 44°17′34.85″N–10°29′51.70″E). (E) Surfaces of localized slip (red arrow) showing different degree of folding: straighter versus folded—note the typical "crust" developed on the surface of the Apennine scaly clays preventing a clear view of the scaly fabric details; this crust is ~1 cm thick (Baiso, Italy; 44°30′34.69″N–10°37′29.31″E).

PROCESSES

Structural observations indicate that scaly fabric is the product of time-dependent permanent deformation that fluctuates between brittle and ductile behavior (Moore et al., 1986; Vannucchi et al., 2003).

Microstructural observations have identified at least four concurrent major mechanisms that can play a role in scaly fabric formation:

1. The first mechanism is independent particulate flow. Borradaile (1981) suggested that particulate flow evolves from independent and/or fluidized to controlled, and to completely coupled; the latter two can also involve cataclasis. In independent particulate flow, grains slip and roll past each other without internal deformation. To do so, the aggregate must be able to dilate, interlock, and rotate (Tarling and Rowe, 2016). Dilation implies a concurrent increase in shear strength against the normal load, and this can endure until fracturing and frictional sliding starts to develop (Houlsby, 1994). Loss of porosity and particle interlocking associated with grain rotation implies that progressive deformation requires the nucleation of new slip surfaces. Scaly fabric formation processes therefore migrate from the already deformed volumes into undeformed clay-rich sediments (Moore et al., 1986). This tendency to involve new, undeformed volumes rather than localize slip also has been observed in analogue models of scaly fabric reproduced using lentils (Tarling and Rowe, 2016). In these experiments, progressive shear did not develop

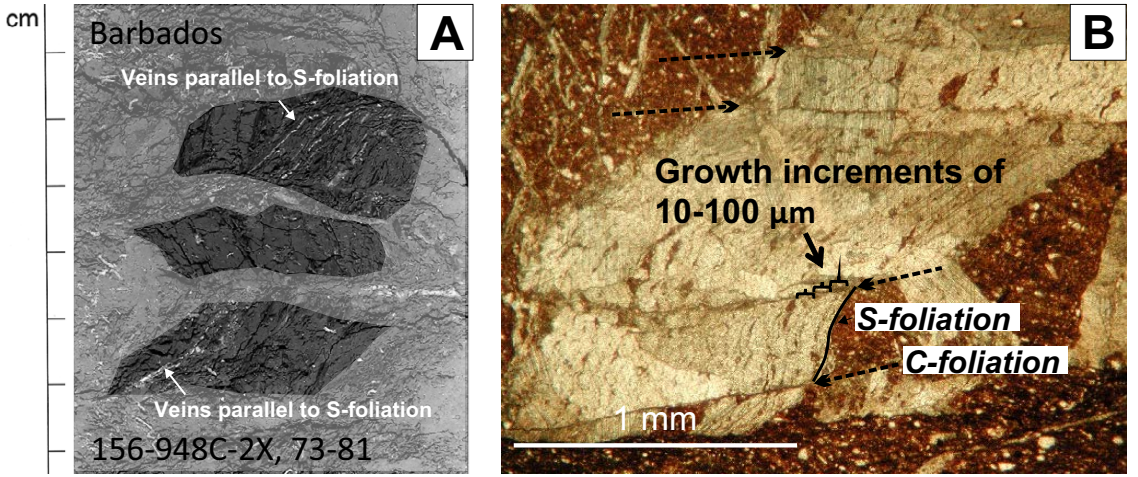

Figure 5. (A) Carbonate veins parallel to the S-foliation recovered within the Barbados décollement (15°32′11.88″N–58°42′50.85″W)—the light-gray area is covering drilling-disturbed parts of the core. (B) Crack-and-seal calcite vein developed parallel to the S-foliation along the veins shown in Figure 4C; dashed lines show C-foliation (Gova, Italy; 44°17′34.85″N–10°29′51.70″E).

localized and through-going slip surfaces, but rather a constant delocalization of deformation with new and transient slip surfaces nucleating where porosity is the greatest. With increasing confining pressure, and according to fluid pressure and strain rate, clay particle size reduction will eventually dominate over particulate flow (Borradaile, 1981). At high strain rates, the volume of comminuted particles retaining fluids could be mobilized through fluidization (Ujiie et al., 2013).

2. The second mechanism is related to slip along preferentially aligned phyllosilicate minerals. Slip can occur both by lattice distortion and edge dislocation according to a mechanism of dislocation creep, producing plastic deformation (Schleicher et al., 2010) and by frictional sliding, producing brittle deformation (den Hartog and Spiers, 2014). Dislocation creep tends to develop in sediments with a high concentration of smectite (Schleicher et al., 2010) and at relatively lower strain rates (and/or higher temperature [T]), while frictional sliding is activated at relatively higher strain rates (and/or lower T) (Fagereng and den Hartog, 2017). Frictional sliding can occur also along non-optimally oriented surfaces or in a highly interlocked fabric—like some anastomosing networks.
3. The third mechanism is related to dilation and compaction and/or pressure solution. In scaly clays, dilation can occur by several processes that range from the release of residual strain during unloading (Prior and Behrmann, 1990), to the volume change observed during shear deformation (Reynolds dilatancy), to slip on curved anastomosing scaliness. Fluid pressure effects are also important and will be specifically discussed below. Compaction and pressure solution, however, are the processes that can accommodate large deformations (Niemeijer and Spiers, 2005; Schleicher et al., 2010; Gratier et al., 2011) and are viable mechanisms for stable creep (Bos and Spiers, 2002). These deformation mechanisms are stress driven. As for pressure solution, fluids assist these mass transfer processes. Pressure solution can operate in two opposite ways to produce coating on phacoids—by concentrating insoluble minerals with pressure-solution diffusion accommodating particle sliding (Gratier et al., 2011) or by authigenic mineral precipitation (Schleicher et al., 2010).
4. The last mechanism for scaly fabric development is related to cyclic variations of pore-fluid pressure (Moore et al., 1986; Labaume et al., 1997b; Vannucchi et al., 2003; Meneghini and Moore, 2007; Vannucchi et al., 2010). The three mechanisms described above can occur at different stages within each pore-pressure cycle. For example, shear-related compactional strain is typical of underconsolidated sediments during stages of relatively low pore pressure (Moore et al., 1986; Meneghini and Moore, 2007). These conditions can be associated with the development of compaction and/or pressure solution and the formation of S-surfaces. The decreasing porosity and the change in permeability conditions can cause overpressure and dilation of already formed S-surfaces. During this stage, compactional strain (pore collapse) is inhibited by high pore pressure, but according to Hubbert and Rubey (1959), displacement at the shear-zone boundaries, here represented by C-surfaces, is likely to be facilitated. Hydrofracturing and extensional failure would then promote pulses of fluid injection along the megathrusts. Episodic fluid flow could redistribute heat and dissolved elements within the sediment volume, promoting chemical processes that could lead to mineral precipitation and fault strengthening during the interseismic period and allow successive hydrofracturing to occur.

The cyclic change from a non-dilatant to dilatant mode of deformation can induce slip instability (i.e., earthquakes). The occurrence of transient fluid-flow advection associated with earthquakes has been suggested by temperature monitoring of the Japan Trench plate boundary fault (Fulton and Brodsky, 2016). In this case, the scaly clays of the plate boundary décollement seem to respond to overpressure in a way that affects fault stability and which may be involved in the triggering of seismic slip.

Scaly fabric is, therefore, the byproduct of the competing deformation modes of continuous viscous deformation and brittle discontinuous deformation. The two types of deformation transition from one into another, occur simultaneously, and/or alternate in time both at the phacoid level and at the outcrop level. This apparent contradiction is also reflected in the interpretation of the seismic processes associated with scaly fabric—either as creep-aseismic processes (Moore et al., 1986) or linked with microseismic activity (Schleicher et al., 2010) and associated with the progressive evolution to localized (seismic) slip (Kirkpatrick et al., 2015).

Frictional Strength of Clay-Rich Sediments and Its Slip Velocity Dependence

Critical elements of scaly fabric are the clay mineral protolith, the fully pervasive geometry, and the polished surfaces. A correct physical model for scaly fabric should adequately explain these features. While it is logical that laboratory experiments will contribute to our understanding of the development of scaly fabric during slip in a clay-rich fault zone, so far, no clay deformation experiment in smectite- and/or illite-rich sediments has been able to generate scaly fabric, i.e., a fabric that satisfies all of the above-mentioned characteristics. In fact, ring-shear experiments using halite and/or kaolinite mixtures, for example, produced a mylonitic S-C microstructure, but without polished surfaces (Bos and Spiers, 2002). This issue will be further addressed in the "future perspective" section of this paper; however, first, we will review key results from experiments that contribute to our current understanding of the necessary preconditions and deformation processes that lead to the development of scaly fabric.

Shear zones in clays have been experimentally produced, starting in the 1960s (Morgenstern and Tchalenko, 1967; Tchalenko, 1968; Maltman, 1977, Carson and Berglund, 1986). Direct shear experiments, for example, focused on reproducing shear-zone geometries. These generated penetrative fabrics in which lenses of less deformed materials are bounded by shear surfaces—but not polished surfaces (Tchalenko, 1968). These experiments clearly illustrated that (1) clay-mineral–preferred orientation is associated with slip (Tchalenko, 1968); (2) there is a wide range of microstructures produced during shearing of clay-rich material, such as Riedel shears, kink bands, crenulations, fractures, etc.; (3) these microstructures can represent incipient stages of cleavage formation (Maltman, 1977; Carson and Berglund, 1986); and (4) these structures can serve as dewatering conduits (Carson and Berglund, 1986). Note that these laboratory experiments were not dynamically scaled to natural fault conditions, in particular in respect to their lack of a high strain and the differing rheological properties of the experimental material.

More recently, laboratory experiments have focused on the frictional characteristics of relevant clays and the relationships between frictional characteristics and slip. Most of these friction experiments were conducted on clay-rich, laboratory-created mixtures, or on natural sediments that originally may have presented a scaly fabric, such as the Tohoku clays (Ujiie et al., 2013); however, these scaly clays were disaggregated and reconstituted prior to testing. Intact fault zone material showing scaly fabric from the Tohoku plate boundary was examined by Ikari et al. (2015a, 2015b). In the following discussion, experiments on samples with or without fabric will be discussed.

In laboratory friction studies, distributed shear is commonly associated with velocity-strengthening behavior (Beeler et al., 1996; Mair and Marone, 1999). This result is compatible with the classic interpretation that scaliness develops volumetrically when clays deform at plate motion speeds (Moore et al., 1986). The anastomosing nature of the network also suggests that multiple scales get activated at the same time, thus allowing distributed slip. However, as scaly fabric develops and evolves, shear zones tend to become more localized. This is recognized by the presence of localized slip surfaces that directly cut or bound scaly fabric intervals—for example, in the Japan Trench décollement drilled during JFAST (Kirkpatrick et al., 2015). Because the experimental transition from distributed deformation to shear localization occurs with the onset of velocity weakening (Beeler et al., 1996; Mair and Marone, 1999), scaly fabric has sometimes also been inferred to be associated with velocity weakening behavior under specific circumstances.

Prompted by the observation that clay-rich fault zones such as megathrusts can support different strain rates with slip velocities ranging from aseismic to seismic, many experiments have been performed to investigate the behavior of clays at different strain rates. Perhaps surprisingly, experiments on clay-rich sediments recovered by scientific drilling projects targeting subduction zones show that, at tectonic plate speeds of 0.001 μm/s, unstable velocity weakening behavior is observed (Ikari et al., 2015a; Ikari and Kopf, 2017). At low, subseismic driving velocities, smectite-rich material shows velocity-neutral or velocity-strengthening behavior (Saffer and Marone, 2003; Ikari et al., 2007; Faulkner et al., 2011; Ferri et al., 2011; Sawai et al., 2014). In high-velocity friction experiments, ≥1 m/s, clay-rich sediments attain localization of deformation and velocity-weakening behavior —the latter probably linked to dynamic weakening mechanisms (Faulkner et al., 2011; Ferri et al., 2011; Ujiie et al., 2013; French et al., 2014; Sawai et al., 2014). In these experiments, the weakening behavior seems to be promoted and/or enhanced by water saturation. In water-saturated experiments, the slip surface is a sub-mm-thick gouge with random orientations of clay-clast aggregates that are sandwiched between two foliated zones. Fragments of the foliated zones can be incorporated into the gouge itself. Injections, fragmentation, and swirls in the gouge also suggest fluidization (Ujiie et al., 2013). Scaly fabric is, therefore, not attained during these experiments, even though it is a major feature of the Tohoku

fault zone, and it should also contribute to further lower fault strength (Bos and Spiers, 2002; Collettini et al., 2009; Ikari et al., 2011). For example, the S-C mylonitic fabric developed during ring-shear experiments on halite and kaolinite mixtures was accompanied by a frictional-viscous behavior (Bos and Spiers, 2002). This observation has been integrated into a model for strength evolution that predicts purely frictional behavior at low and high shear strain rates and frictional-viscous behavior at intermediate shear strain rate (Bos and Spiers, 2002). S-C fabric development could be, therefore, associated with major weakening.

Samples of intact sediments from Tohoku fault zone tested at low sliding velocities (<1 mm/s) are nearly cohesionless, but their friction coefficient is higher than powdered samples from the same interval (Ikari et al., 2015b). This trend was also observed for samples coming from the San Andreas fault (Carpenter et al., 2012). It is interesting to notice that Tohoku scaly fabric is not associated with mineral precipitation (i.e., Kirkpatrick et al., 2015), while along other megathrusts, crack-seal veins are common, particularly along the S-surfaces (Labaume et al., 1997a, 1997b; Vannucchi et al., 2010). In these latter cases, cementation of phacoids would lead to cohesion strengthening occurring during the interseismic stage. Finally, at plate motion strain rate, the intact fault zone material from the Tohoku fault zone shows unstable slip behavior generating an environment frictionally favorable for seismic slip propagation (Ikari and Kopf, 2017).

An interesting finding that can help explain this wide range of behavior is that at relatively low slip rates, experiments on smectite-rich material show the production of amorphous nanoparticles (Aretusini et al., 2017). These particles could play an important role in controlling frictional behavior of faults at high slip rates because they could be more efficient in realizing bond water with the effects of decreasing the temperature for dynamic weakening to occur (Aretusini et al., 2017). In this case, scaly fabric could be a "facilitator" for slip localization and weakening during seismic events.

Samples with scaly fabric, though, could have a more complex rheology. Schleicher et al. (2010) suggest that the smectite-rich coating on phacoids surfaces is responsible for creep and contributes to the weak strength of the scaly clays. In this model, chemically active circulating fluids play a key role in nucleation and mineralization processes along the fracture surfaces. Coatings could represent low-permeability barriers so that small and localized fluid overpressure can build up during slip coupled with dissolution in adjacent volumes. Schleicher et al. (2010) envision a final stage where phacoids interconnect and develop an anastomosing network of low-permeability, clay-sealed fractures susceptible to creep. Considering the anisotropic porosity and permeability with domains of authigenic clay growth and aligned and unaligned clay minerals, this evolution can help the delocalization of deformation by nucleating new slip surfaces. However, the presence of weaker layers can also progress to slip localization along these weakened zones.

The key characteristic of scaly fabric is that it develops polished surfaces. This aspect remains the most elusive to attain in laboratory experiments, and the examples are not directly related to clay-rich material. In the laboratory, shiny sliding surfaces are produced: by sintered wear particles in sandstone (Hirose et al., 2012); by the formation of finely comminuted, amorphous, wet silica gel on the sliding surface in diorite and quartzite (Goldsby and Tullis, 2002; Di Toro et al., 2004); or by nanometric particles in carbonates (Tisato et al., 2012; Chen et al., 2013; Smith et al., 2013; Verberne et al., 2013). The development of nanometric particles is observed to occur both at low and high slip velocity with a difference of "continuity": shiny slip surfaces formed at subseismic velocities are patchy (Verberne et al., 2014), while those formed at coseismic velocity are more continuous (Fondriest et al., 2013). Although the above-mentioned sets of experiments were not performed on clay-rich materials, an interesting observation coming from them is that, with the development of a shiny localized slip surface, the rate of frictional wear is greatly reduced (Hirose et al., 2012), and a "dynamic" velocity-weakening behavior is established (Oohashi et al., 2011; Smith et al., 2013).

FUTURE PERSPECTIVES

Among the different questions raised in the spectrum of studies on scaly fabric, those of primary interest include:

Can Scaly Fabric Be Reproduced in Laboratory Experiments?

In spite of its common occurrence in nature and seemingly across the whole spectrum of slip speeds that occur along faults from creep to slow slip to earthquake, scaly fabric is particularly hard to replicate in laboratory experiments. Our ability to develop laboratory methods for the investigation of clay-rich sediments has increased substantially in the past 15 years, as has our understanding of the behavior of clay-rich sediments; but scaly fabric remains an elusive structure. Its development is now thought to be a function of effective stress, volumetric strain, and strain rate. Our difficulties in reproducing scaly fabric may lie in the fact that scaly fabric may form at low strain rates (or alternating low strain-rate and high strain-rate conditions?) that are not typically accessed in the laboratory, or that it is formed by interactions between multiple processes that have yet to the reproduced in laboratory experiments. Scaly fabric has also been proposed to involve mass transfer processes such as pressure solution (Bos et al., 2000) and precipitation (Schleicher et al., 2010), and these processes pose experimental challenges. Foliation and tectonic layering has been reproduced experimentally on a mixture of plaster and phyllosilicates during a uniaxial long-term experiment, with local dissolution of the plaster concentrating the phyllosilicates along thin layers surrounding phacoids of intact material (Gratier et al., 2015). Phyllosilicate segregation into a distinct foliation was also attained during high-velocity rotary friction experiments on a clay-bearing, carbonate-hosted fault, suggesting a coseismic origin (Smeraglia et al., 2017). A mylonitic fabric has been reproduced for a mixture of kaolinite and halite saturated with brines and deformed at high strain, low

strain rate, and low-temperature conditions in a rotary apparatus (Bos et al., 2000; Bos and Spiers, 2000, 2002). These latter experiments showed a significant strain weakening and a transition from stress-sensitive to rate-sensitive deformation. On the opposite side, fault materials that preserve scaly fabric show higher friction coefficients and lower cohesion than the same material disaggregated and reconstituted (Ikari et al., 2015b; Ikari and Kopf, 2017). These are promising ways to investigate the behavior of networks of anastomosing fabric that experience simple shear.

Polished mirror-like surfaces were produced in the laboratory in dolostone only for seismic slip rates (~1 m/s) (Fondriest et al., 2013), however discontinuous shiny surfaces were produced at subseismic velocity in simulated calcite fault gauge (Veberne et al., 2014). In carbonates, smooth sliding surfaces are attributed to the presence of nanometric particles (Fondriest et al., 2012; Verberne et al., 2013; Verberne et al., 2014). Although not directly comparable, nanoparticles of amorphous silica were also produced during experiments on smectite-rich material (Aretusini et al., 2017). Understanding the role of smectite-rich polished surfaces typical of scaly fabric remains a challenge with hints, such as the similarity with mirror-like smoothness (Sagy et al., 2007), that they might be critical to accommodate unstable slip. The mechanism producing these surfaces in clay-rich materials still needs critical input from laboratory experiments. In addition, the influence of phyllosilicate foliation and polished surfaces on subsequent deformation is an area where there are no data, because preserving the scaly fabric of natural samples while performing experiments on them still remains a technical challenge. This area of analyses should become a prime experimental focus, if we aim to decipher the fingerprints and the conditions that underlie aseismic and seismic slip.

Scaly Fabric, Localized Shear, and Their Intermediate States: What Is Their Relationship?

Scaly clays are associated with heterogeneous mechanical and physical properties and heterogeneous fluid conditions that promote alternation between shear failure and viscoplastic flow and distributed and localized slip. These competing deformation modes may underlie geophysically observed strain release variations in the shallow portions of subduction megathrusts that range from continuous aseismic creep to episodic seismic slip. Seismic, hydrogeologic, and geodetic monitoring of subduction zones such as the Japan Trench (Fukao and Kanjo, 1980; Fujiwara et al., 2011; Ito et al., 2011; Ito et al., 2013; Ito et al., 2015; Fulton and Brodsky, 2016) and Costa Rica (Brown et al., 2005; DeShon et al., 2006; Walter et al., 2011; Walter et al., 2013; Xue et al., 2015; Jiang et al., 2017) shows that these different mechanisms to accommodate displacement can coexist at the depths where scaly fabric has been cored (Tobin et al., 2001; Chester et al., 2013) and in regions where scaly fabric characterizes the state of the sediments delivered to depth, since scaly fabric develops early in the evolution of a shear zone and, therefore, can influence its subsequent deformation.

Why Does Scaly Fabric Deform at a Wide Range of Slip Velocities?

Creep, slow slip events, and earthquake ruptures are complex phenomena that alternate in time and space along the portions of active faults where scaly fabric has been collected, such as the Japan Trench (Chester et al., 2013; Kirkpatrick et al., 2015) and the San Andreas fault (Schleicher et al., 2006; Schleicher et al., 2010; Gratier et al., 2011; Richard et al., 2014). Scaly fabric has been observed within creeping sections of crustal faults (Schleicher et al., 2006) and along faults that have had recent and observed seismic rupture propagation (Chester et al., 2013).

The in situ development of scaly fabric can introduce enough heterogeneity in clays to locally and temporarily alter their frictional properties. Over-pressured migrating fluids, different smoothness and 3D interconnections of the slip surfaces, and the distribution of healing phases, e.g., mineralized veins, can all create strong heterogeneities within the rock mass. Frictional properties and strength can also be altered more "directly," and their relationship is not clear. Experiments show that S-C fabric is promoting frictional-viscous behavior and increased weakness of fault zones (Bos and Spiers, 2002) but also friction coefficients higher than in undeformed sediments accompanied by lower cohesion—effectively cohesionless material (Ikari et al., 2015b).

Veins associated with scaly fabric are commonly parallel to flattening bands. The veins show growth intervals representing slip on the order of 10–100 μm (Vannucchi et al., 2010). This geometry and these slip increments suggest shear failure at low effective normal stress within a heterogeneous medium. Shear failure at low effective normal stress is often thought to be the triggering mechanism for tremors (Fisher and Brantley, 2014; Ujiie et al., 2018). Tremors are swarms of low- and very low frequency seismic events (Thomas et al., 2009). In Costa Rica, tremors are documented to occur at a shallow level from the trench (Walter et al., 2011, 2013). This level is at ~2 km below the sea floor in the region where scaly clay has been drilled along the décollement at ~0.35 km from the sea floor (Vannucchi and Tobin, 2000; Tobin et al., 2001).

CONCLUSIONS

Scaly fabric is a common, visually striking feature within many different environments in which clay-rich sediments have been mobilized or deformed. It is a mesoscopic descriptive term for a rock fabric that is penetratively cut by anastomosing polished surfaces. At the microscopic scale, scaly fabric appears to be formed of combinations of flattening bands and/or dissolution surfaces, fractures, and shear surfaces. These structures appear possible to develop under conditions that range from brittle to ductile processes; within fault zones, scaly fabric also seems to be able to accommodate and/or respond to a wide range of geologic processes.

The presence of scaly fabric in fault systems that cut through clay-rich sediments is overwhelming. It appears to develop early on as clays begin to deform and is particularly common at shallow subduction plate boundaries

in which the whole spectrum of slip speeds from creep to slow slip to earthquake rupture propagation has been documented by geophysical monitoring. The implication of its ubiquitous presence, in agreement with microstructural observations, is that a scaly fabric can be produced easily in natural environments and that it can host a variety of slip rates. The processes that create and develop scaly fabric may therefore be fundamental and relate to shear failure in a rock assemblage that has a mixed rheology as the byproduct of previous progressive deformation. In this case, scaly fabric could be the critical structure that promotes frictional transitions in shear behavior and the occurrence of shear failure within fault zones that have a bulk viscoplastic rheology.

The evolution of a clay-rich sediment as it develops scaly fabric still needs to be integrated into a concrete model of fabric evolution that can be constrained by experimental data. In the classic model, the increase in fluid pressure caused by tectonic stress applied to unconsolidated and/or low-permeability sediments is what triggers failure, followed by collapse and local strengthening as fluid is expelled (e.g., Moore et al., 1986). This model assumes that failure planes are abandoned after limited slip with deformation shifting to an adjacent failure surface, and it is therefore insufficient to explain slip concentration and the wide range of conditions under which scaly fabric can exist. Also, experiments on intact fault material with scaly fabric imply that a clay-rich sediment in which phacoids have developed behaves like cohesionless granular material. Cohesion strengthening is, on the contrary, suggested if veining is found associated with scaly fabric. In this scenario, strength variation would be controlled by cohesion rather than by friction changes with a key role played by the environmental conditions—pressure, temperature, and time—and geochemistry of circulating fluids. Clay phacoids seem therefore to be the key mechanical units that we need to study, in terms of their influence on mechanical—frictional versus cohesion changes—and seismic behavior—fault slip stability.

ACKNOWLEDGMENTS

The author wishes to thank J.P Gratier, an anonymous reviewer, and the editor P. Agard for their suggestions and comments, which greatly improved the paper. The author also thanks S. Angiboust for the invitation to contribute to the ST2B-2 themed issue of *Geosphere*; F. Remitti for providing the photograph in Figure 4A; and Jason Morgan for his critical reading of the text.

REFERENCES CITED

Agar, S.M., Prior, D.J., and Behrmann, J.H., 1989, Back-scattered electron imagery of the tectonic fabrics of some fine-grained sediments: Implications for fabric nomenclature and deformation processes: Geology, v. 17, p. 901–904, https://doi.org/10.1130/0091-7613(1989)017<0901:BSEIOT>2.3.CO;2.

Aretusini, S., Mittempergher, S., Plümper, O., Spagnuolo, E., Gualtieri, A., and Di Toro, G., 2017, Production of nanoparticles during experimental deformation of smectite and implications for seismic slip: Earth and Planetary Science Letters, v. 463, p. 221–231, https://doi.org/10.1016/j.epsl.2017.01.048.

Beeler, N.M., Tullis, T.E., Blanpied, M.L., and Weeks, J.D., 1996, Frictional behavior of large displacement experimental faults: Journal of Geophysical Research, v. 101, no. B4, p. 8697–8715, https://doi.org/10.1029/96JB00411.

Bennett, R.H., Bryant, W.R., and Hulbert, M.H., 1991, Determinants of clay and shale microfabric signatures: Processes and mechanisms, *in* Bennett, R.H., Bryant, W.R., and Hulbert, M.H., eds., Microstructure of Fine-Grained Sediments: From Mud to Shale: Berlin, Springer, p. 5–32, https://doi.org/10.1007/978-1-4612-4428-8_2.

Bettelli, G., and Vannucchi, P., 2003, Structural style of the offscraped Ligurian oceanic sequences of the Northern Apennines: New hypothesis concerning the development of mélange block-in-matrix fabric: Journal of Structural Geology, v. 25, no. 3, p. 371–388, https://doi.org/10.1016/S0191-8141(02)00026-3.

Bianconi, P., 1840, Storia naturale dei terreni ardenti, dei vulcani fangosi, delle sorgenti infiammabili, dei pozzi idropirici e di altri fenomeni geologici oprati dal gas idrogeno e dell'origine di esso gas: Bologna, Marsigli, 164 p.

Borradaile, G.J., 1981, Particulate flow of rock and the formation of cleavage: Tectonophysics, v. 72, p. 305–321, https://doi.org/10.1016/0040-1951(81)90243-2.

Bos, B., and Spiers, C.J., 2000, Effect of phyllosilicates on fluid-assisted healing of gouge-bearing faults: Earth and Planetary Science Letters, v. 184, no. 1, p. 199–210, https://doi.org/10.1016/S0012-821X(00)00304-6.

Bos, B., and Spiers, C.J., 2002, Frictional-viscous flow of phyllosilicate-bearing fault rock: Microphysical model and implications for crustal strength profiles: Journal of Geophysical Research. Solid Earth, v. 107, no. B2, p. ECV1–ECV13.

Bos, B., Peach, C.J., and Spiers, C.J., 2000, Frictional-viscous flow of simulated fault gouge caused by the combined effects of phyllosilicates and pressure solution: Tectonophysics, v. 327, no. 3–4, p. 173–194, https://doi.org/10.1016/S0040-1951(00)00168-2.

Brantley, S., Fisher, D.M., Clark, M.B., Myers, G., and Deines, P., 1997, Segregation veins: Evidence for the deformation and dewatering of a low-grade metapelite, *in* Holness, M.B., ed., Deformation-Enhanced Fluid Transport in the Earth's Crust and Mantle: London, Chapman and Hall, p. 266–287.

Brown, K.M., Tryon, M.D., DeShon, H.R., Dorman, L.M., and Schwartz, S.Y., 2005, Correlated transient fluid pulsing and seismic tremor in the Costa Rica subduction zone: Earth and Planetary Science Letters, v. 238, no. 1–2, p. 189–203, https://doi.org/10.1016/j.epsl.2005.06.055.

Byrne, T., 1984, Early deformation in mélange terrains of the Ghost Rock Formation, Kodiak Island Alaska, *in* Raymond, L.A., ed., Mélanges: Their Nature, Origin and Significance: Geological Society of America Special Paper 198, p. 21–52, https://doi.org/10.1130/SPE198-p21.

Carpenter, B.M., Saffer, D.M., and Marone, C., 2012, Frictional properties and sliding stability of the San Andreas fault from deep drill core: Geology, v. 40, p. 759–762, https://doi.org/10.1130/G33007.1.

Carson, B., and Berglund, P.L., 1986, Sediment deformation and dewatering under horizontal compression: Experimental results, *in* Moore, J.C., ed., Structural Fabrics in Deep Sea Drilling Project Cores from Forearcs: Geological Society of America Memoir 166, p. 135–150, https://doi.org/10.1130/MEM166-p135.

Casciello, E., Cesarano, M., and Cosgrove, J.W., 2004, Shear deformation of pelitic rocks in a large-scale natural fault, *in* Alsop, G.I., Holdsworth, R.E., McCaffrey, K.J.W., and Hand, M., eds., Flow Processes in Faults and Shear Zones: Geological Society of London Special Publication 224, p. 113–125, https://doi.org/10.1144/GSL.SP.2004.224.01.08.

Chen, X.F., Madden, A.S., Bickmore, B.R., and Reches, Z., 2013, Dynamic weakening by nanoscale smoothing during high-velocity fault slip: Geology, v. 41, no. 7, p. 739–742, https://doi.org/10.1130/G34169.1.

Chester, F. M., Mori, J. J., Toczko, S., Eguchi, N., and the Expedition 343/343T Scientists, 2012, Japan Trench Fast Drilling Project (JFAST): Tokyo, Integrated Ocean Drilling Program, Management International, Inc., Preliminary Reports, v. 343 and 343T, https://doi.org/10.2204/iodp.proc.343343T.2013.

Chester, F.M., Rowe, C., Ujiie, K., Kirkpatrick, J., Regalla, C., Remitti, F., Moore, J.C., Toy, V., Wolfson-Schwehr, M., Bose, S., Kameda, J., Mori, J.J., Brodsky, E.E., Eguchi, N., Toczko, S., Expedition, S., and Expedition, T.S., 2013, Structure and composition of the plate-boundary slip zone for the 2011 Tohoku-Oki earthquake: Science, v. 342, no. 6163, p. 1208–1211, https://doi.org/10.1126/science.1243719.

Collettini, C., Niemeijer, A., Viti, C., and Marone, C., 2009, Fault zone fabric and fault weakness: Nature, v. 462, p. 907–910, https://doi.org/10.1038/nature08585.

Cowan, D.S., 1985, Structural styles in Mesozoic and Cenozoic mélanges in the western Cordillera of North America: Geological Society of America Bulletin, v. 96, p. 451–462, https://doi.org/10.1130/0016-7606(1985)96<451:SSIMAC>2.0.CO;2.

Dellisanti, F., Pini, G.A., Tateo, F., and Baudin, F., 2008, The role of tectonic shear strain on the illitization mechanism of mixed-layers illite-smectite. A case study from a fault zone in the Northern Apennines, Italy: International Journal of Earth Sciences, v. 97, no. 3, p. 601–616, https://doi.org/10.1007/s00531-007-0180-4.

den Hartog, S.A.M., and Spiers, C.J., 2014, A microphysical model for fault gouge friction applied to subduction megathrusts: Journal of Geophysical Research. Solid Earth, v. 119, no. 2, p. 1510–1529, https://doi.org/10.1002/2013JB010580.

DeShon, H.R., Schwartz, S.Y., Newman, A.V., Gonzalez, V., Protti, M., Dorman, L.R.M., Dixon, T.H., Sampson, D.E., and Flueh, E.R., 2006, Seismogenic zone structure beneath the Nicoya Peninsula, Costa Rica, from three-dimensional local earthquake P- and S-wave tomography: Geophysical Journal International, v. 164, no. 1, p. 109–124, https://doi.org/10.1111/j.1365-246X.2005.02809.x.

Di Toro, G., Goldsby, D.L., and Tullis, T.E., 2004, Friction falls towards zero in quartz rock as slip velocity approaches seismic rates: Nature, v. 427, no. 6973, p. 436–439, https://doi.org/10.1038/nature02249.

Elliott, S.J., Fisher, D.M., Ukar, E., Ramirez, G., and Forstner, S., 2017, Slip behavior of a subduction zone: Preliminary inferences from quartz and calcite filled veins (hydrofractures) in an exhumed accretionary wedge, Shimanto Belt, Japan: Geological Society of America Abstracts with Programs, v. 49, no. 6, p. 254–258.

Fagereng, A., 2011, Geology of the seismogenic subduction thrust interface, *in* Fagereng, A., Toy, V., and Rowland, J.V., eds., Geology of the Earthquake Source: A Volume in Honour of Rick Sibson: Geological Society of London Special Publication 359, p. 55–76, https://doi.org/10.1144/SP359.4.

Fagereng, A., and den Hartog, S.A.M., 2017, Subduction megathrust creep governed by pressure solution and frictional-viscous flow: Nature Geoscience, v. 10, no. 1, p. 51–57, https://doi.org/10.1038/ngeo2857.

Fagereng, A., Remitti, F., and Sibson, R., 2011, Incrementally developed slickenfibers—Geological record of repeating low stress-drop seismic events?: Tectonophysics, v. 510, p. 381–386, https://doi.org/10.1016/j.tecto.2011.08.015.

Faulkner, D.R., Mitchell, T.M., Behnsen, J., Hirose, T., and Shimamoto, T., 2011, Stuck in the mud?: Earthquake nucleation and propagation through accretionary forearcs: Geophysical Research Letters, v. 38, 5 p., https://doi.org/10.1029/2011GL048552.

Ferri, F., Di Toro, G., Hirose, T., Han, R., Noda, H., Shimamoto, T., Quaresimin, M., and de Rossi, N., 2011, Low- to high-velocity frictional properties of the clay-rich gouges from the slipping zone of the 1963 Vaiont slide, northern Italy: Journal of Geophysical Research. Solid Earth, v. 116, B09208, https://doi.org/10.1029/2011JB008338.

Fisher, D.M., and Brantley, S.L., 2014, The role of silica redistribution in the evolution of slip instabilities along subduction interfaces: Constraints from the Kodiak accretionary complex, Alaska: Journal of Structural Geology, v. 69, p. 395–414, https://doi.org/10.1016/j.jsg.2014.03.010.

Fisher, D.M., Smye, A., Marone, C., and Yamaguchi, A., 2017, Record of slow slip instabilities in rocks: The role of silica redistribution in the behavior of subduction interfaces: Proceedings Subduction Interface Processes: Barcelona [abs.], p. 14.

Fondriest, M., Smith, S.A.F., Di Toro, G., Zampieri, D., and Mittempergher, S., 2012, Fault zone structure and seismic slip localization in dolostones, an example from the Southern Alps, Italy: Journal of Structural Geology, v. 45, p. 52–67, https://doi.org/10.1016/j.jsg.2012.06.014.

Fondriest, M., Smith, S.A.F., Candela, T., Nielsen, S.B., Mair, K., and Di Toro, G., 2013, Mirror-like faults and power dissipation during earthquakes: Geology, v. 41, no. 11, p. 1175–1178, https://doi.org/10.1130/G34641.1.

French, M.E., Kitajima, H., Chester, J.S., Chester, F.M., and Hirose, T., 2014, Displacement and dynamic weakening processes in smectite-rich gouge from the Central Deforming Zone of the San Andreas fault: Journal of Geophysical Research. Solid Earth, v. 119, no. 3, p. 1777–1802, https://doi.org/10.1002/2013JB010757.

Fujiwara, T., Kodaira, S., No, T., Kaiho, Y., Takahashi, N., and Kaneda, Y., 2011, The 2011 Tohoku-Oki earthquake: Displacement reaching the trench axis: Science, v. 334, no. 6060, p. 1240, https://doi.org/10.1126/science.1211554.

Fukao, Y., and Kanjo, K., 1980, A zone of low-frequency earthquakes beneath the inner wall of the Japan Trench: Tectonophysics, v. 67, p. 153–162, https://doi.org/10.1016/0040-1951(80)90170-5.

Fulton, P.M., and Brodsky, E.E., 2016, In situ observations of earthquake-driven fluid pulses within the Japan Trench plate boundary fault zone: Geology, v. 44, no. 10, p. 851–854, https://doi.org/10.1130/G38034.1.

Goldsby, D.L., and Tullis, T.E., 2002, Low frictional strength of quartz rocks at subseismic slip rates: Geophysical Research Letters, v. 29, no. 17, https://doi.org/10.1029/2002GL015240.

Gratier, J.P., Richard, J., Renard, F., Mittempergher, S., Doan, M.L., Di Toro, G., Hadizadeh, J., and Boullier, A.M., 2011, Aseismic sliding of active faults by pressure solution creep: Evidence from the San Andreas Fault Observatory at Depth: Geology, v. 39, no. 12, p. 1131–1134, https://doi.org/10.1130/G32073.1.

Gratier, J.-P., Noiriel, C., and Renard, F., 2015, Experimental evidence for rock layering development by pressure solution: Geology, v. 43, no. 10, p. 871–874, https://doi.org/10.1130/G36713.1.

Hashimoto, Y., Eida, M., Kirikawa, T., Iida, R., Takagi, M., Furuya, M., Nikaizo, A., Kikuchi, T., and Yoshimitsu, T., 2012, Large amount of fluid migration around shallow seismogenic depth preserved in tectonic mélange: Yokonami mélange, the Cretaceous Shimanto Belt, Kochi, Southwest Japan: The Island Arc, v. 21, p. 53–64, https://doi.org/10.1111/j.1440-1738.2011.00806.x.

Hirose, T., Mizoguchi, K., and Shimamoto, T., 2012, Wear processes in rocks at slow to high slip rates: Journal of Structural Geology, v. 38, p. 102–116, https://doi.org/10.1016/j.jsg.2011.12.007.

Houlsby, G.T., 1994, How the dilatancy of soils affects their behavior: Firenze, Associazione Geotecnica Italiana, Deformation of Soils and Displacements of Structures, p. 1189–1202.

Hubbert, M.K., and Rubey, W.W., 1959, Role of fluid pressure in mechanics of overthrust faulting: Geological Society of America Bulletin, v. 70, p. 115–160, https://doi.org/10.1130/0016-7606(1959)70[115:ROFPIM]2.0.CO;2.

Ikari, M.J., and Kopf, A.J., 2017, Seismic potential of weak, near-surface faults revealed at plate tectonic slip rates: Science Advances, v. 3, no. 11, e1701269, https://doi.org/10.1126/sciadv.1701269.

Ikari, M.J., Saffer, D.M., and Marone, C., 2007, Effect of hydration state on the frictional properties of montmorillonite-based fault gouge: Journal of Geophysical Research. Solid Earth, v. 112, B06423, https://doi.org/10.1029/2006JB004748.

Ikari, M.J., Marone, C., and Saffer, D.M., 2011, On the relation between fault strength and frictional stability: Geology, v. 39, p. 83-86, https://doi.org/10.1130/G31416.1.

Ikari, M.J., Ito, Y., Ujiie, K., and Kopf, A.J., 2015a, Spectrum of slip behaviour in Tohoku fault zone samples at plate tectonic slip rates: Nature Geoscience, v. 8, no. 11, p. 870, https://doi.org/10.1038/ngeo2547.

Ikari, M.J., Kameda, J., Saffer, D.M., and Kopf, A.J., 2015b, Strength characteristics of Japan Trench borehole samples in the high-slip region of the 2011 Tohoku-Oki earthquake: Earth and Planetary Science Letters, v. 412, p. 35–41, https://doi.org/10.1016/j.epsl.2014.12.014.

Ito, Y., Tsuji, T., Osada, Y., Kido, M., Inazu, D., Hayashi, Y., Tsushima, H., Hino, R., and Fujimoto, H., 2011, Frontal wedge deformation near the source region of the 2011 Tohoku-Oki earthquake: Geophysical Research Letters, v. 38, https://doi.org/10.1029/2011GL048355.

Ito, Y., Hino, R., Kido, M., Fujimoto, H., Osada, Y., Inazu, D., Ohta, Y., Iinuma, T., Ohzono, M., Miura, S., Mishina, M., Suzuki, K., Tsuji, T., and Ashi, J., 2013, Episodic slow slip events in the Japan subduction zone before the 2011 Tohoku-Oki earthquake: Tectonophysics, v. 600, p. 14–26, https://doi.org/10.1016/j.tecto.2012.08.022.

Ito, Y., Hino, R., Suzuki, S., and Kaneda, Y., 2015, Episodic tremor and slip near the Japan Trench prior to the 2011 Tohoku-Oki earthquake: Geophysical Research Letters, v. 42, no. 6, p. 1725–1731, https://doi.org/10.1002/2014GL062986.

Jiang, Y., Liu, Z., Davis, E.E., Schwartz, S.Y., Dixon, T.H., Voss, N., Malservisi, R., and Protti, M., 2017, Strain release at the trench during shallow slow slip: The example of Nicoya Peninsula, Costa Rica: Geophysical Research Letters, v. 44, no. 10, p. 4846–4854, https://doi.org/10.1002/2017GL072803.

Kimura, G., Silver, E.A., Blum, P., et al., eds., 1997, Proceedings of the Ocean Drilling Program, Initial Report, 170: College Station, Texas, Ocean Drilling Program, 458 p.

Kirkpatrick, J.D., Rowe, C.D., Ujiie, K., Moore, J.C., Regalla, C., Remitti, F., Toy, V., Wolfson-Schwehr, M., Kameda, J., Bose, S., and Chester, F.M., 2015, Structure and lithology of the Japan Trench subduction plate boundary fault: Tectonics, v. 34, no. 1, p. 53–69, https://doi.org/10.1002/2014TC003695.

Kondo, H., Kimura, G., Masago, H., Ohmori-Ikehara, K., Kitamura, Y., Ikesawa, E., Sakaguchi, A., Yamaguchi, A., and Okamoto, S., 2005, Deformation and fluid flow of a major out-of-sequence thrust located at seismogenic depth in an accretionary complex: Nobeoka Thrust in the Shimanto Belt, Kyushu, Japan: Tectonics, v. 24, TC6008, https://doi.org/10.1029/2004TC001655.

Labaume, P., Kastner, M., Trave, A., and Henry, P., 1997a, Carbonate veins from the decollement zone at the toe of the Northern Barbados accretionary prism: Microstructure, mineralogy, geochemistry, and relations with prism structures and fluid regime, *in* Shipley, T.H., Ogawa, Y., Blum, P., and Bahr, J.M., eds., Proceedings of the Ocean Drilling Program, Scientific Results, Volume 156: College Station, Texas, Ocean Drilling Program, p. 79–96.

Labaume, P., Maltman, A., Bolton, A., Tessier, D., Ogawa, Y., and Takizawa, S., 1997b, Scaly fabrics in sheared clays from the décollement zone of the Barbados accretionary prism, *in* Shipley, T.H., Ogawa, Y., Blum, P., and Bahr, J.M., eds., Proceedings of the Ocean Drilling Program, Scientific Results, Volume 156: College Station, Texas, Ocean Drilling Program, p. 59–77.

Lister, G., and Snoke, A., 1984, S-C mylonites: Journal of Structural Geology, v. 6, p. 617–638, https://doi.org/10.1016/0191-8141(84)90001-4.

Mair, K., and Marone, C., 1999, Friction of simulated fault gouge for a wide range of velocities and normal stresses: Journal of Geophysical Research. Solid Earth, v. 104, no. B12, p. 28899–28914, https://doi.org/10.1029/1999JB900279.

Maltman, A., Labaume, P., and Housen, B., 1997, Structural geology of the décollement at the toe of the Barbados accretionary prism, *in* Shipley, T.H., Ogawa, Y., Blum, P., and Bahr, J.M., eds., Proceedings of the Ocean Drilling Program, Scientific Results, Volume 156: College Station, Texas, Ocean Drilling Program, p. 279–292.

Maltman, A.J., 1977, Some microstructures of experimentally deformed argillaceous sediments: Tectonophysics, v. 39, p. 417–436, https://doi.org/10.1016/0040-1951(77)90107-X.

Maltman, A.J., and Vannucchi, P., 2004, Insights from the Ocean Drilling Program on shear and fluid-flow at the mega-faults between actively converging plates, *in* Alsop, G.I., Holdsworth, R.E., McCaffrey, K.J.W., and Hand, M., eds., Flow Processes in Faults and Shear Zones: Geological Society of London Special Publication 224, https://doi.org/10.1144/GSL.SP.2004.224.01.09.

Maltman, A.J., Byrne, T., Karig, D.E., Lallemant, S., Knipe, R., and Prior, D.J., 1993, Deformation structures at Site 808, Nankai accretionary prism, Japan, *in* Hill, I.A., Taira, A., and Firth, J.V., eds., Proceedings of the Ocean Drilling Program, Initial Report 131: College Station, Texas, Ocean Drilling Program, p. 123–133.

Mascle, A., Moore, J.C., et al., 1988, Proceedings of the Ocean Drilling Program, Initial Report 110: College Station, Texas, Ocean Drilling Program, https://doi.org/10.2973/odp.proc.ir.110.1988.

Matsumura, M., Hashimoto, Y., Kimura, G., Ohmori-Ikehara, K., Enjohji, M., and Ikesawa, E., 2003, Depth of oceanic-crust underplating in a subduction zone: Inferences from fluid-inclusion analyses of crack-seal vein: Geology, v. 31, p. 1005–1008, https://doi.org/10.1130/G19885.1.

Meneghini, F., and Moore, J.C., 2007, Deformation and hydrofracture in a subduction thrust at seismogenic depths: The Rodeo Cove thrust zone, Marin Headlands, California: Geological Society of America Bulletin, v. 119, p. 174–183, https://doi.org/10.1130/B25807.1.

Moore, G.F., Taira, A., Klaus, A., et al., 2001, Proceedings of the Ocean Drilling Program, Initial Report 190: College Station, Texas, Ocean Drilling Program, https://doi.org/10.2973/odp.proc.ir.190.2001.

Moore, J.C., Roeske, S., Cowan, D.S., Lundberg, N., Gonzales, E., Schoonmaker, J., and Lucas, S.E., 1986, Scaly fabrics from Deep Sea Drilling Project cores from forearcs, *in* Moore, J.C., ed., Structural Fabrics in Deep Sea Drilling Project Cores from Forearcs: Geological Society of America Memoir 166, p. 55–74, https://doi.org/10.1130/MEM166-p55.

Morgenstern, N.R., and Tchalenko, J.S., 1967, Microscopic structures in kaolin subjected to direct shear: Geotechnique, v. 17, p. 309–328, https://doi.org/10.1680/geot.1967.17.4.309.

Morris, J.D., Villinger, H.W., Klaus, A., et al., eds., 2003, Proceedings of the Ocean Drilling Program, Initial Report 205: College Station, Texas, Ocean Drilling Program, 75 CD-ROM p.

Nadeau, R.M., and McEvilly, T.V., 2004, Periodic pulsing of characteristic microearthquakes on the San Andreas fault: Science, v. 303, no. 5655, p. 220–222, https://doi.org/10.1126/science.1090353.

Niemeijer, A.R., and Spiers, C.J., 2005, Influence of phyllosilicates on fault strength in the brittle-ductile transition: Insights from rock analogue experiments, *in* Bruhn, D., and Burlini, L., eds., High-Strain Zones: Structure and Physical Properties: Geological Society of London Special Publication 245, p. 303–327, https://doi.org/10.1144/GSL.SP.2005.245.01.15.

Oohashi, K., Hirose, T., and Shimamoto, T., 2011, Shear-induced graphitization of carbonaceous materials during seismic fault motion: Experiments and possible implications for fault mechanics: Journal of Structural Geology, v. 33, no. 6, p. 1122–1134, https://doi.org/10.1016/j.jsg.2011.01.007.

Prior, D.J., and Behrmann, J.H., 1990, Thrust-related mudstone fabrics from the Barbados forearc: A backscattered scanning electron microscope study: Journal of Geophysical Research, v. 95, p. 9055–9067, https://doi.org/10.1029/JB095iB06p09055.

Ramirez, G.E., Fisher, D.M., Smye, A., Hashimoto, Y., and Yamaguchi, A., 2017, Scaly fabrics and veins of tectonic mélanges in the Shimanto Belt, SW Japan, *in* Proceedings of the American Geophysical Union, Fall Meeting 2017, abstract no. T41D-0653.

Rice, J.R., 2006, Heating and weakening of faults during earthquake slip: Journal of Geophysical Research, v. 111, B05311, https://doi.org/10.1029/2005JB004006.

Richard, J., Gratier, J.P., Doan, M.L., Boullier, A.M., and Renard, F., 2014, Rock and mineral transformations in a fault zone leading to permanent creep: Interactions between brittle and viscous mechanisms in the San Andreas fault: Journal of Geophysical Research. Solid Earth, v. 119, no. 11, p. 8132–8153, https://doi.org/10.1002/2014JB011489.

Saffer, D.M., and Marone, C., 2003, Comparison of smectite- and illite-rich gouge frictional properties: Application to the updip limit of the seismogenic zone along subduction megathrusts: Earth and Planetary Science Letters, v. 215, no. 1–2, p. 219–235, https://doi.org/10.1016/S0012-821X(03)00424-2.

Saffer, D.M., and Wallace, L.M., 2015, The frictional, hydrologic, metamorphic and thermal habitat of shallow slow earthquakes: Nature Geoscience, v. 8, no. 8, p. 594–600, https://doi.org/10.1038/ngeo2490.

Sagy, A., Brodsky, E.E., and Axen, G., 2007, Evolution of fault-surface roughness with slip: Geology, v. 35, no. 3, p. 283–286, https://doi.org/10.1130/G23235A.1.

Satake, K., Fujii, Y., Harada, T., and Namegaya, Y., 2013, Time and space distribution of coseismic slip of the 2011 Tohoku earthquake as inferred from tsunami waveform data: Bulletin of the Seismological Society of America, v. 103, no. 2B, p. 1473–1492, https://doi.org/10.1785/0120120122.

Sawai, M., Hirose, T., and Kameda, J., 2014, Frictional properties of incoming pelagic sediments at the Japan Trench: Implications for large slip at a shallow plate boundary during the 2011 Tohoku earthquake: Earth, Planets, and Space, v. 66, https://doi.org/10.1186/1880-5981-66-65.

Schleicher, A.M., van der Pluijm, B.A., Solum, J.G., and Warr, L.N., 2006, Origin and significance of clay-coated fractures in mudrock fragments of the SAFOD borehole (Parkfield, California): Geophysical Research Letters, v. 33, no. 16, L16313, https://doi.org/10.1029/2006GL026505.

Schleicher, A.M., van der Pluijm, B.A., and Warr, L.N., 2010, Nanocoatings of clay and creep of the San Andreas fault at Parkfield, California: Geology, v. 38, no. 7, p. 667–670, https://doi.org/10.1130/G31091.1.

Shervais, J.W., Choi, S.H., Sharp, W.D., Ross, J., Zoglman-Schuman, M., and Mukasa, S.B., 2011, Serpentinite matrix mélange: Implications of mixed provenance for mélange formation, *in* Wakabayashi, J., and Dilek, Y., eds., Mélanges: Processes of Formation and Societal Significance: Geological Society of America Special Paper 480, p. 1–30, https://doi.org/10.1130/2011.2480(01).

Sibson, R.H., 1990, Conditions for fault-valve behavior, *in* Knipe, R.J., and Rutter, E.H., eds., Deformation Mechanisms, Rheology and Tectonics: Geological Society of London Special Publication 54, p. 15–28.

Smeraglia, L., Bettucci, A., Billi, A., Carminati, E., Cavallo, A., Di Toro, G., Natali, M., Passeri, D., Rossi, M., and Spagnuolo, E., 2017, Microstructural evidence for seismic and aseismic slips along clay-bearing, carbonate faults: Journal of Geophysical Research. Solid Earth, v. 122, no. 5, p. 3895–3915, https://doi.org/10.1002/2017JB014042.

Smith, S.A.F., Di Toro, G., Kim, S., Ree, J.H., Nielsen, S., Billi, A., and Spiess, R., 2013, Coseismic recrystallization during shallow earthquake slip: Geology, v. 41, no. 1, p. 63–66, https://doi.org/10.1130/G33588.1.

Taira, A., Hill, I., Firth, J.V., et al., 1991, Proceedings of the Ocean Drilling Program, Initial Reports, Vol. 131: College Station, Texas, Ocean Drilling Program, 285 p., https://doi.org/10.2973/odp.proc.ir.131.1991.

Tarling, M.S., and Rowe, C.D., 2016, Experimental slip distribution in lentils as an analog for scaly clay fabrics: Geology, v. 44, no. 3, p. 183–186, https://doi.org/10.1130/G37306.1.

Tchalenko, J.S., 1968, The evolution of kink-bands and the development of compression textures in sheared clays: Tectonophysics, v. 6, p. 159–174, https://doi.org/10.1016/0040-1951(68)90017-6.

Thomas, A.M., Nadeau, R.M., and Burgmann, R., 2009, Tremor-tide correlations and near-lithostatic pore pressure on the deep San Andreas fault: Nature, v. 462, no. 7276, p. 1048–1051, https://doi.org/10.1038/nature08654.

Tisato, N., Di Toro, G., De Rossi, N., Quaresimin, M., and Candela, T., 2012, Experimental investigation of flash weakening in limestone: Journal of Structural Geology, v. 38, p. 183–199, https://doi.org/10.1016/j.jsg.2011.11.017.

Titus, S.J., DeMets, C., and Tikoff, B., 2006, Thirty-five-year creep rates for the creeping segment of the San Andreas fault and the effects of the 2004 Parkfield earthquake: Constraints from alignment arrays, continuous global positioning system, and creepmeters: Bulletin of the Seismological Society of America, v. 96, no. 4B, p. S250–S268, https://doi.org/10.1785/0120050811.

Tobin, H., Vannucchi, P., and Meschede, M., 2001, Structure, inferred mechanical properties, and implications for fluid transport in the decollement zone, Costa Rica convergent margin: Geology, v. 29, no. 10, p. 907–910, https://doi.org/10.1130/0091-7613(2001)029<0907:SIMPAI>2.0.CO;2.

Ujiie, K., Tanaka, H., Saito, T., Tsutsumi, A., Mori, J.J., Kameda, J., Brodsky, E.E., Chester, F.M., Eguchi, N., Toczko, S., and Expedition 343 and 343T Scientists, 2013, Low coseismic shear stress on the Tohoku-Oki megathrust determined from laboratory experiments: Science, v. 342, no. 6163, p. 1211–1214, https://doi.org/10.1126/science.1243485.

Ujiie, K., Saishu, H., Fagereng, A., Nishiyama, N., Otsubo, M., Masuyama, H., and Kagi, H., 2018, An explanation of episodic tremor and slow slip constrained by crack-seal veins and viscous shear in subduction mélanges: Geophysical Research Letters, v. 45, p. 5371–5379, https://doi.org/10.1029/2018GL078374.

Vannucchi, P., and Bettelli, G., 2002, Mechanisms of subduction accretion as implied from the broken formations in the Apennines, Italy: Geology, v. 30, no. 9, p. 835–838, https://doi.org/10.1130/0091-7613(2002)030<0835:MOSAAI>2.0.CO;2.

Vannucchi, P., and Leoni, L., 2007, Structural characterization of the Costa Rica decollement: Evidence for seismically-induced fluid pulsing: Earth and Planetary Science Letters, v. 262, no. 3–4, p. 413–428, https://doi.org/10.1016/j.epsl.2007.07.056.

Vannucchi, P., and Tobin, H., 2000, Deformation structures and implications for fluid flow at the Costa Rica convergent margin, ODP Sites 1040 and 1043, Leg 170: Journal of Structural Geology, v. 22, no. 8, p. 1087–1103, https://doi.org/10.1016/S0191-8141(00)00027-4.

Vannucchi, P., Maltman, A., Bettelli, G., and Clennell, B., 2003, On the nature of scaly fabric and scaly clay: Journal of Structural Geology, v. 25, no. 5, p. 673–688, https://doi.org/10.1016/S0191-8141(02)00066-4.

Vannucchi, P., Remitti, F., Bettelli, G., Boschi, C., and Dallai, L., 2010, Fluid history related to the early Eocene–middle Miocene convergent system of the Northern Apennines (Italy): Constraints from structural and isotopic studies: Journal of Geophysical Research. Solid Earth, v. 115, 23 p., B05405, https://doi.org/10.1029/2009JB006590.

Verberne, B.A., de Bresser, J.H.P., Niemeijer, A.R., Spiers, C.J., de Winter, D.A.M., and Plumper, O., 2013, Nanocrystalline slip zones in calcite fault gouge show intense crystallographic preferred orientation: Crystal plasticity at sub-seismic slip rates at 18–150 °C: Geology, v. 41, no. 8, p. 863–866, https://doi.org/10.1130/G34279.1.

Verberne, B.A., Plumper, O., de Winter, D.A.M., and Spiers, C.J., 2014, Superplastic nanofibrous slip zones control seismogenic fault friction: Science, v. 346, no. 6215, p. 1342–1344, https://doi.org/10.1126/science.1259003.

Vrolijk, P.J., Myers, G., and Moore, J.C., 1988, Warm fluid migration along tectonic mélanges in the Kodiak Accretionary Complex, Alaska: Journal of Geophysical Research, v. 93, p. 10,313–10324, https://doi.org/10.1029/JB093iB09p10313.

Wallace, L.M., Webb, S.C., Ito, Y., Mochizuki, K., Hino, R., Henrys, S., Schwartz, S.Y., and Sheehan, A.F., 2016, Slow slip near the trench at the Hikurangi subduction zone, New Zealand: Science, v. 352, no. 6286, p. 701–704, https://doi.org/10.1126/science.aaf2349.

Wallace, L.M., Kaneko, Y., Hreinsdottir, S., Hamling, I., Peng, Z.G., Bartlow, N., D'Anastasio, E., and Fry, B., 2017, Large-scale dynamic triggering of shallow slow slip enhanced by overlying sedimentary wedge: Nature Geoscience, v. 10, no. 10, p. 765, https://doi.org/10.1038/ngeo3021.

Walter, J.I., Schwartz, S.Y., Protti, J.M., and Gonzalez, V., 2011, Persistent tremor within the northern Costa Rica seismogenic zone: Geophysical Research Letters, v. 38, L01307, https://doi.org/10.1029/2010GL045586.

Walter, J.I., Schwartz, S.Y., Protti, M., and Gonzalez, V., 2013, The synchronous occurrence of shallow tremor and very low frequency earthquakes offshore of the Nicoya Peninsula, Costa Rica: Geophysical Research Letters, v. 40, no. 8, p. 1517–1522, https://doi.org/10.1002/grl.50213.

Xue, L., Schwartz, S., Liu, Z., and Feng, L.J., 2015, Interseismic megathrust coupling beneath the Nicoya Peninsula, Costa Rica, from the joint inversion of InSAR and GPS data: Journal of Geophysical Research. Solid Earth, v. 120, no. 5, p. 3707–3722, https://doi.org/10.1002/2014JB011844.